SUPPLEMENTAL INFORMATION

Compromised Mechanical Homeostasis in Arterial Aging and Associated Cardiovascular Consequences

J. Ferruzzi[1,*], D. Madziva[1], A.W. Caulk[1], G. Tellides[2,3], J.D. Humphrey[1,2]

[1]Department of Biomedical Engineering
Yale University, New Haven, CT, USA

[2]Vascular Biology and Therapeutics Program and [3]Department of Surgery
Yale School of Medicine, New Haven, CT, USA

[*]Currently: Department of Biomedical Engineering,
Boston University, Boston, MA, USA

Address for Correspondence:

J.D. Humphrey, Ph.D.
Department of Biomedical Engineering
Malone Engineering Center
Yale University
55 Prospect Street
New Haven, CT, 06520 USA
jay.humphrey@yale.edu

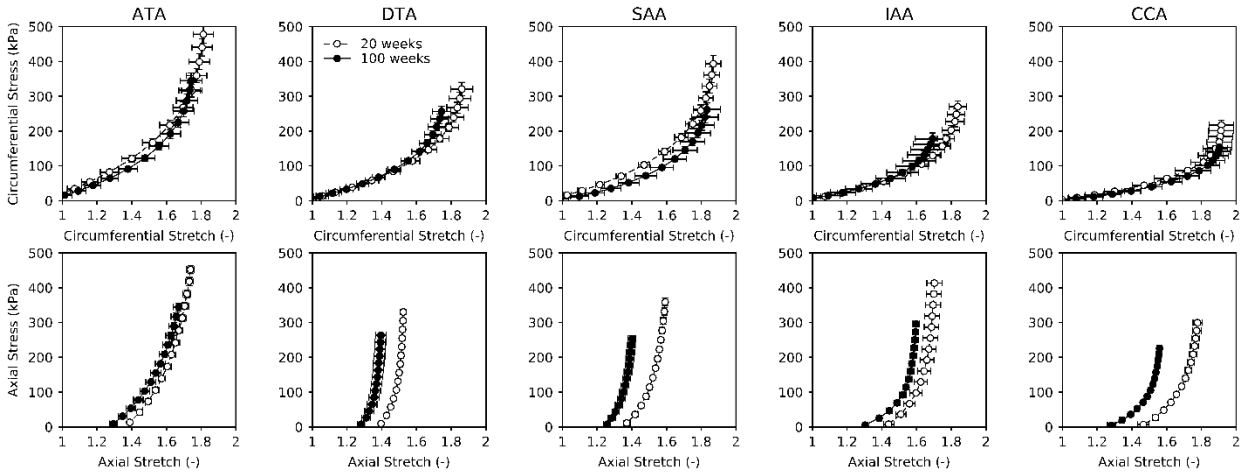

Figure S1. Mean ± SEM biaxial Cauchy stress-stretch behaviors measured as a function of age (20 vs. 100 weeks) across five key central arteries: ascending thoracic aorta (ATA), descending thoracic aorta (DTA), suprarenal abdominal aorta (SAA), infrarenal abdominal aorta (IAA), and common carotid artery (CCA). Circumferential properties measured at the individually estimated values of in vivo axial stretch (top row) are surprisingly unaffected by aging while axial properties measured at a common distending pressure of 100 mmHg (bottom row) suggest material stiffening.

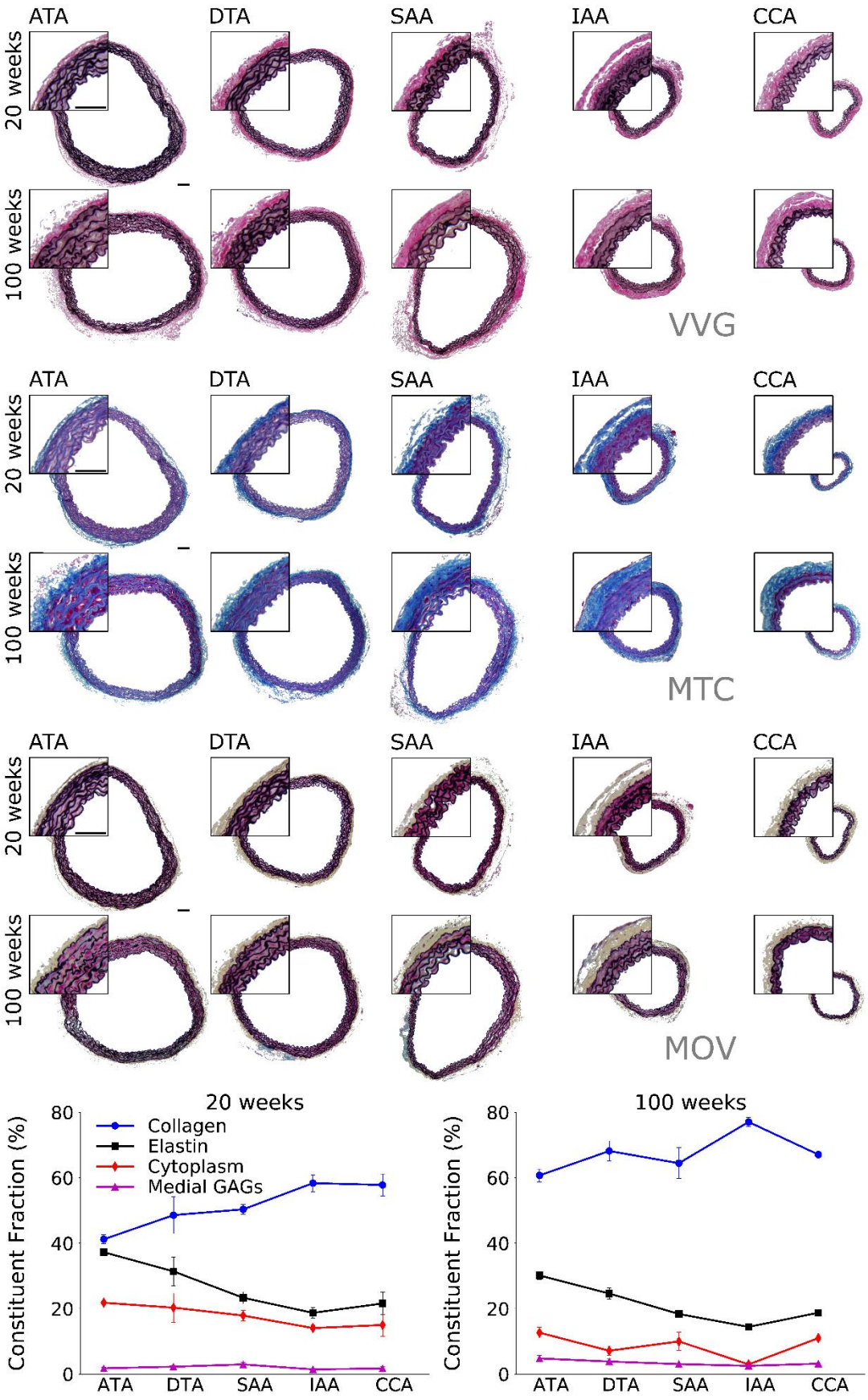
ATA
DTA
SAA
IAA
CCA
20 weeks
100 weeks
VVG
MTC
MOV
20 weeks
100 weeks
Constituent Fraction (%)
Collagen
Elastin
Cytoplasm
Medial GAGs
0
20
40
60
80
ATA
DTA
SAA
IAA
CCA

Figure S2. (previous page) Microstructural composition at 20- and 100-weeks of age for the five regions of interest: ATA, DTA, SAA, IAA, and CCA. Representative images from Verhoeff Van Gieson (VVG, first row), Masson's Trichrome (MTC, second row), and Movat's Pentachrome (MOV, third row) show both entire cross-sections and zoomed-in details. Scale bars represent 100 μm. Regional variations in area fractions of individual constituents (fourth row): elastin, fibrillar collagen, cytoplasm, and medial glycosaminoglycans (GAGs) are shown separately for the two ages. Overall, aged vessels show a general increase in collagen and decrease in cytoplasm, as revealed as an increase of blue stain and decrease in red stain in MTC images. Medial GAGs, quantified from MOV images, increase mainly in the ATA and IAA.

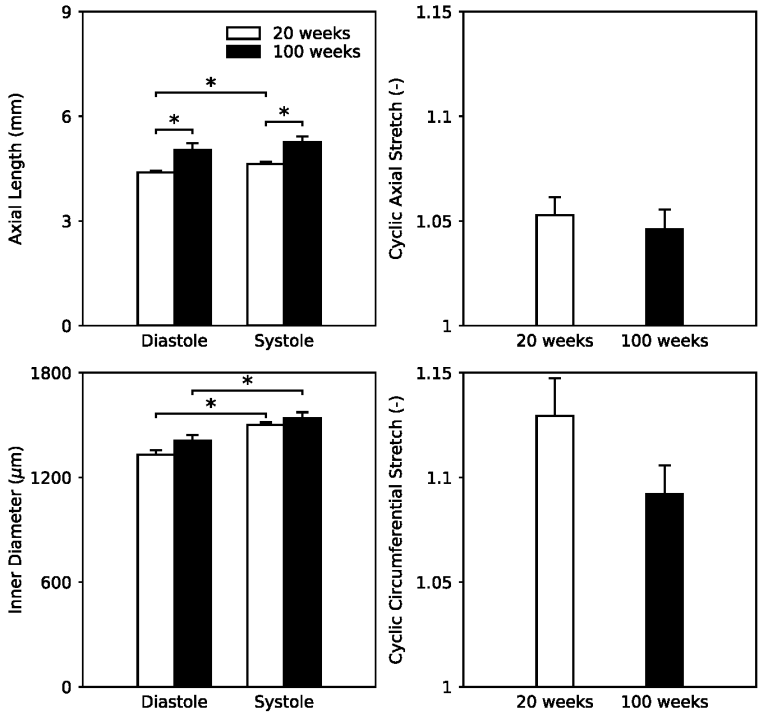

Figure S3. In vivo biaxial motions (left column) and computed stretches (right column) for the ascending thoracic aorta (ATA) measured under isoflurane anesthesia using a high-frequency Vevo 2100 system (Visualsonics, Toronto, Canada). Non-invasive B-Mode imaging and speckle-tracking reveal changes in axial length and inner diameter over a cardiac cycle and thus enable computation of cyclic biaxial stretches (i.e., systolic relative to diastolic). Analysis of axial motions (top row) reveals an increased ATA length at systole and diastole due to normal aging, yet cyclic axial stretches are nearly preserved. Analysis of circumferential motions (bottom row) confirms that the inner diameter is essentially unaffected by aging, but cyclic circumferential stretch is decreased – albeit not significantly ($p < 0.2$) – which supports findings from M-Mode measurements (cf. Figure S4).

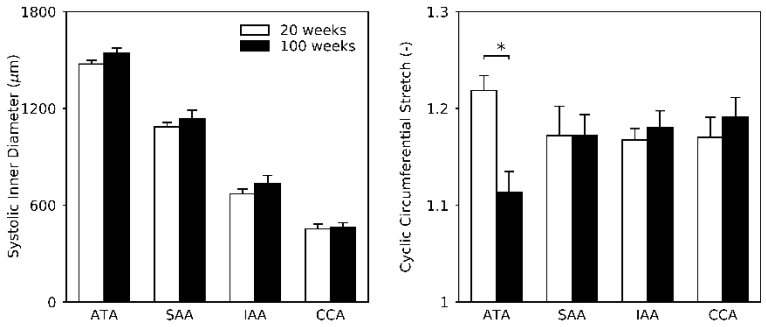

Figure S4. Regional inner diameters at systole (left) and associated cyclic circumferential stretches (right) measured in vivo under isoflurane anesthesia using a high-frequency Vevo 2100 system (Visualsonics, Toronto, Canada). Non-invasive M-Mode imaging and custom automatic image analysis allows inner diameter to be tracked and cyclic circumferential stretches to be computed, thus indicating extents of arterial deformation at systole with respect to diastole. Note that, of the five regions of interest, the DTA could not be monitored in vivo due to shadowing caused by air in the adjacent lungs. Systolic inner diameter is preserved with aging, while cyclic circumferential stretch is decreased in the ATA alone.

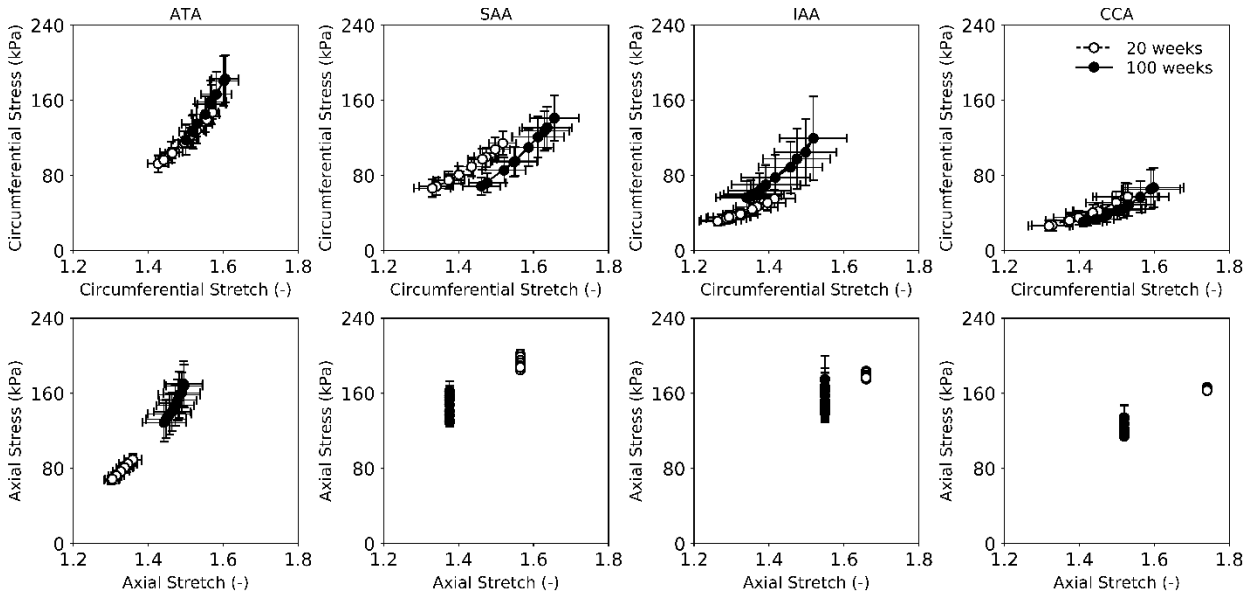

Figure S5. In vivo biaxial stress-stretch behaviors, under anesthesia, obtained by combining material properties quantified in vitro with motions measured in vivo using ultrasound imaging. Due to its unique biaxial motions, we used inner diameter and length measured with B-Mode imaging for the ATA; in contrast, we used M-Mode imaging for the SAA, IAA, and CCA since it appears that they each have a fixed axial length equal to the energetically optimal value inferred in vitro. Circumferential properties (top row) are preserved while axial properties (bottom row) change with aging. The ATA shows increased stresses due to its increased length, whereas the SAA, IAA, and CCA show a general trend of decreased stretches and stresses.

Table S1. Tabulated values (mean ± SEM) of key geometrical and mechanical metrics as a function of age (20 vs. 100 weeks) and region: ATA, DTA, SAA, IAA, and CCA. Values were computed at individual values of in vivo axial stretch but a common value of transmural pressure (120 mmHg). The * and † indicate significant differences, respectively, at $p < 0.05$ and $p < 0.10$ for vessels from 100-week old mice relative to 20-week old mice. Compare, too, with values listed in Table 2 in Ferruzzi et al. (2015).

	ATA		DTA		SAA		IAA		CCA	
	20 weeks	**100 weeks**	**20 weeks**	**100 weeks**	**20 weeks**	**100 weeks**	**20 weeks**	**100 weeks**	**20 weeks**	**100 weeks**
n	5	6	5	5	5	5	5	6	5	5
Unloaded Dimensions										
Outer Diameter (μm)	1090 ± 22	1113 ± 27	827 ± 17	883 ± 15*	832 ± 9	820 ± 23	588 ± 9	622 ± 22	409 ± 11	408 ± 9
Wall Thickness (μm)	105 ± 1	125 ± 4*	105 ± 3	112 ± 2†	92 ± 4	111 ± 3*	91 ± 3	110 ± 2*	84 ± 4	96 ± 4†
In-vitro Axial Length (mm)	3.4 ± 0.1	3.5 ± 0.2	5.8 ± 0.2	7.7 ± 0.3*	5.7 ± 0.2	6.7 ± 0.6	5.2 ± 0.4	7.1 ± 0.1*	5.2 ± 0.2	6.5 ± 0.1*
Systolic Dimensions										
Outer Diameter (μm)	1783 ± 38	1722 ± 38	1357 ± 28	1367 ± 27	1386 ± 25	1316 ± 30	929 ± 16	890 ± 29	642 ± 3	613 ± 9*
Wall Thickness (μm)	35 ± 0.5	46 ± 2*	38 ± 0.4	47 ± 1*	32 ± 1	45 ± 1*	30 ± 2	43 ± 1*	26 ± 1	34 ± 1*
Inner Radius (μm)	857 ± 19	815 ± 18	640 ± 14	636 ± 14	661 ± 13	613 ± 15*	434 ± 9	402 ± 14†	296 ± 3	272 ± 4*
In-vivo Axial Stretch	1.71 ± 0.02	1.62 ± 0.03*	1.50 ± 0.01	1.38 ± 0.03*	1.56 ± 0.01	1.37 ± 0.02*	1.66 ± 0.04	1.55 ± 0.02*	1.73 ± 0.03	1.52 ± 0.02*
Systolic Cauchy Stresses (kPa)										
Circumferential	395.9 ± 6.0	287.2 ± 8.9*	268.1 ± 8.4	214.9 ± 9.4*	330.1 ± 14.8	217.9 ± 6.6*	230.4 ± 16.0	149.9 ± 4.6*	186.7 ± 12.1	128.5 ± 5.2*
Axial	377.7 ± 4.6	278.0 ± 5.7*	251.2 ± 8.7	218.6 ± 11.9†	299.3 ± 16.9	197.8 ± 8.8*	275.1 ± 13.9	202.4 ± 6.5*	228.7 ± 21.1	165.5 ± 3.4*
Systolic Stiffness (MPa)										
Circumferential	2.57 ± 0.10	2.00 ± 0.08*	1.81 ± 0.09	1.45 ± 0.06*	2.30 ± 0.07	1.59 ± 0.07*	1.86 ± 0.15	1.06 ± 0.04*	1.87 ± 0.22	1.07 ± 0.08*
Axial	2.53 ± 0.05	1.79 ± 0.05*	4.21 ± 0.50	4.15 ± 0.35	3.35 ± 0.19	2.60 ± 0.2*	4.08 ± 0.22	2.91 ± 0.21*	3.94 ± 0.83	2.86 ± 0.28
Systolic Stored Energy (kPa)	108.7 ± 1.8	75.6 ± 2.3*	64.4 ± 2.6	47.1 ± 3.7*	84.0 ± 4.1	46.7 ± 2.2*	61.2 ± 5.4	38.9 ± 1.5*	54.3 ± 4.0	34.3 ± 1*
Energy Dissipation Ratio (%)	1.89 ± 0.56	3.17 ± 0.28†	3.90 ± 1.04	5.05 ± 0.11	3.84 ± 0.36	5.69 ± 0.54*	5.84 ± 0.85	5.09 ± 0.57	4.54 ± 0.71	6.34 ± 0.41†
Opening Angle (deg)	68.4 ± 7.5	102.8 ± 8.9*	25.5 ± 10.7	21.1 ± 11.6	95.0 ± 16.0	53.7 ± 20.3	71.3 ± 29.1	53.4 ± 19.1	18.3 ± 4.3	-9.0 ± 6.6*
Distensibility (mmHg^{-1})	0.0028 ± 0.0002	0.0026 ± 0.0001	0.0028 ± 0.0003	0.0028 ± 0.0001	0.0026 ± 0.0001	0.0024 ± 0.0001	0.0021 ± 0.0001	0.0027 ± 0.0001*	0.0019 ± 0.0003	0.0023 ± 0.0002

Table S2. Best-fit mean values of the parameters in the four-fiber family constitutive model for central arteries excised from 20-week and 100-week old mice for the 5 regions of interest: ATA, DTA, SAA, IAA, and CCA. The RMSE (root mean square of the error) from the nonlinear regression was less than 0.09 for all regions and both ages, thus indicating good theoretical fits to the combined (7 protocols) biaxial data-sets, accomplished separately for each region and age.

		Elastic Fibers	Axial Collagen		Circumferential Collagen + SMC		Symmetric Diagonal Collagen			Error
		c (kPa)	c_1^1 (kPa)	c_2^1	c_1^2 (kPa)	c_2^2	$c_1^{3,4}$ (kPa)	$c_2^{3,4}$	α_0 (deg)	*RMSE*
20 weeks	ATA	26.159	16.653	0.080	14.881	0.081	4.729	0.433	44.055	0.079
	DTA	20.377	15.952	0.536	12.218	0.112	0.045	2.796	26.545	0.073
	SAA	29.056	22.659	0.119	10.194	0.136	0.420	1.350	31.233	0.058
	IAA	12.634	16.888	0.162	10.748	0.124	0.035	1.682	29.394	0.077
	CCA	8.073	17.084	0.069	8.854	0.056	0.000	2.643	35.089	0.085
100 weeks	ATA	24.854	18.642	0.001	8.808	0.220	5.269	0.535	40.910	0.052
	DTA	21.817	15.069	1.273	12.428	0.174	0.536	3.704	21.434	0.063
	SAA	18.231	32.579	0.272	7.878	0.160	1.287	2.356	25.636	0.050
	IAA	15.725	3.982	0.810	8.276	0.197	1.209	1.215	31.042	0.083
	CCA	10.731	21.869	0.166	4.059	0.114	0.005	3.149	27.172	0.079

Table S3. Blood pressure and heart rate measured non-invasively using a CODA tail-cuff system (Kent Scientific Corporation, Torrington, CT) under conscious conditions at rest in 20-week vs. 100-week old wild-type male mice. Pulse pressure is increased in aged animals due to a decrease in diastolic pressure. The * and † indicate significant differences, respectively, at $p < 0.05$ and $p < 0.10$, between 20- and 100-week old animals.

	20 weeks	100 weeks
n	10	6
Blood Pressure (mmHg)		
Systolic	120 ± 6	107 ± 6
Mean	96 ± 6	78 ± 5†
Diastolic	84 ± 6	64 ± 5*
Pulse	36 ± 1	42 ± 3*
Heart Rate (bpm)	692 ± 19	731 ± 18

Table S4. Blood pressure and heart rate measured invasively using a Millar SPR-1000 catheter (Millar, Houston, TX) under isoflurane anesthesia in 20-week vs. 100-week old wild-type male mice. Pulse pressure shows a statistically significant increase in aged animals. The * indicates significant differences, at $p < 0.05$, between 20- and 100-week old animals.

	20 weeks	100 weeks
n	5	5
Blood Pressure (mmHg)		
Systolic	99 ± 2	102 ± 3
Mean	79 ± 2	79 ± 3
Diastolic	69 ± 2	68 ± 3
Pulse	30 ± 1	35 ± 1*
Heart Rate (bpm)	459 ± 15	555 ± 16*

Table S5. Hemodynamic measurements under isoflurane anesthesia using a Vevo 2100 system with pulsed-wave Doppler. Peak velocity at systole increased significantly in both the ascending (ATA) and infrarenal (IAA) regions of the aorta due to normal aging. The time lag between blood velocity waveforms measured at the aortic root and the iliac bifurcation, known as the pulse transit time, was ~40% lower due to aging, suggesting a faster wave propagation even though the difference did not reach statistical significance. The * indicates significant differences, at $p < 0.05$, between 20- and 100-week old animals.

	20 weeks	**100 weeks**
n	5	6
Peak Velocity (cm/s)		
ATA	107 ± 13	148 ± 11*
IAA	29 ± 5	51 ± 7*
Pulse Transit Time (ms)	12.3 ± 2.4	7.7 ± 2.2